

Relationship between Molecular Structure and Electron Targets in the Electroreduction of Benzocarbazolediones and Anilinenaphthoquinones. Experimental and Theoretical Study

N. Macías-Ruvalcaba,[†] G. Cuevas,[†] I. González,[‡] and M. Aguilar-Martínez^{*,†}

Instituto de Química, Universidad Nacional Autónoma de México, Ciudad Universitaria, 04510 México D.F., Mexico, and Departamento de Química, Universidad Autónoma Metropolitana-Iztapalapa, Apartado Postal 55-534, 09340 México D.F., Mexico

marthaa@servidor.unam.mx

Received November 19, 2001

We report the synthesis and voltamperometric reduction of 5H-benzo[b]carbazole-6,11-dione (BCD) and its 2-R-substituted derivatives (R = –OMe, –Me, –COMe, –CF₃). The electrochemical behavior of BCDs was compared to that of the 2-[(R-phenyl)amine]-1,4-naphthalenediones (PANs) previously studied. Like PANs, BCDs exhibit two reduction waves in acetonitrile. The first reduction step for the BCDs represents formation of the radical anion, and the half-wave potential ($E_{1/2}$) values for this step are less negative than for that of the PANs. The second reduction wave, corresponding to the formation of dianion hydroquinone, has $E_{1/2}$ values that shift to more negative potentials. A good linear Hammett–Zuman ($E_{1/2}$ vs σ_p) relationship, similar to that for the PAN series, was also obtained for the BCDs. However, unlike the PANs, in the BCDs, the first reduction wave was more susceptible to the effect of the substituent groups than was the second wave, suggesting that the ordering of the two successive one-electron reductions in BCDs is opposite that in PANs. This is explained by the fact that the electron delocalizations in the two systems are different; in the case of BCDs there is an extra aromatic indole ring, which resists loss of its aromatic character. The electronic structures of BCD compounds were, therefore, investigated within the framework of the density functional theory, using the B3LYP hybrid functional with a double ζ split valence basis set. Our theoretical calculations show that the O₁...H–N hydrogen bond, analogous to that previously described for the PAN series, is not observed in the BCDs. Laplacians of the critical points ($\nabla^2\rho$) and the natural charges for the C–O bonds indicate that the first reduction wave for the BCDs corresponds to the C₄–O₂ carbonyl, while in the PAN series the first one-electron transfer occurred at the C₁–O₁ carbonyl. Natural bond orbital analysis showed that, in all the BCDs, the lowest unoccupied molecular orbital (LUMO) is located at C₄, whereas for the PANs, the LUMO is found at C₁. The good correlation between the LUMO energy values and the $E_{1/2}$ potentials (wave I) established that the first one-electron addition takes place at the LUMO. Analysis of the molecular geometry confirmed that, in both series of compounds, the effect of the substituent groups is mainly on the C₄–O₂ carbonyl. These results explain the fact that reduction of the C₄–O₂ carbonyl (voltammetric wave II in the PANs and voltammetric wave I in the BCDs) is more susceptible to the effect of the substituent groups than is reduction of the C₁–O₁ carbonyl (wave I in the PANs and wave II in the BCDs).

Introduction

Organic molecules containing a quinone moiety are important in a wide variety of biological activities.¹ Many such molecules are used pharmaceutically as agents against tuberculosis,² malaria,³ bacterial infections,⁴ and tumor growth,⁵ in water management and agriculture to combat larvae,⁶ in mollusk infestations,⁶ and as herbi-

cides⁷ and fungicides.⁸ The biological activity of the quinoid compounds is reportedly due to the redox chemistry of the quinone system.^{1,9} Quinones are capable of accepting one or two electrons to form the corresponding radical anion (Q^{•-}) and hydroquinone dianion (Q²⁻). These species interact with crucial cellular molecules such as oxygen, DNA, and proteins, altering and possibly controlling their biological activity.^{1,9,10} To effect such

* To whom correspondence should be addressed at the Departamento de Físicoquímica, Facultad de Química, Universidad Nacional Autónoma de México, Ciudad Universitaria, 04510 México D.F., Mexico.

[†] Universidad Nacional Autónoma de México.

[‡] Universidad Autónoma Metropolitana-Iztapalapa.

(1) Morton, R. A., Ed. *Biochemistry of Quinones*; Academic Press: New York, 1965.

(2) Oeriu, I.; Benesch, H. *Bull. Soc. Chim. Biol.* **1962**, *44*, 91–100. Oeriu, I. *Biokhimiya* **1963**, *28*, 380–383.

(3) Prescott, B. *J. Med. Chem.* **1969**, *12*, 181–182.

(4) Silver, R. F.; Holmes, H. L. *Can. J. Chem.* **1968**, *46*, 1859–1864.

(5) Hodnett, E. M.; Wongwiechintana, C.; Dunn, W. J.; Marrs, P. J. *Med. Chem.* **1983**, *26*, 570–574.

(6) Lopez, J. N. C.; Johnson, A. W.; Grove, J. F.; Bulhoes, M. S. *Cienc. Cult. (Sao Paulo)* **1977**, *29*, 1145–1149.

(7) U.S. Rubber Co. British Patent 862 489, 1959. Takeda Chemical Industry Co. Ltd. Japanese Patent 18 520, 1963. Ube Industries Ltd. Japanese Patent 126 725, 1979. Shell Internationale Research Maatschappij B.V. British Patent 1 314 881, 1973.

(8) Clark, N. G. *Pestic. Sci.* **1985**, *16*, 23–32.

(9) (a) Monks, T. J.; Hanzlik, R. P.; Cohen, G. M.; Ross, D.; Graham, D. G. *Toxicol. Appl. Pharmacol.* **1992**, *112*, 2–16. (b) Wolstenholme, G. E. W., O'Connor, C. M., Eds. *Quinones in Electron Transport*; Churchill: London, 1961.

(10) Brunmark, A.; Cadenas, E. *Free Radical Biol. Med.* **1988**, *7*, 435–477.

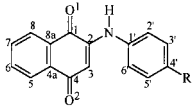
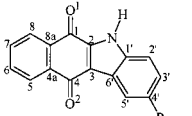
fine-tuned manipulations, the molecules not only must be capable of accepting electrons at some site with appropriate speed and energy, but also should accept electrons in the correct site.¹¹

The chemical and biological importance of quinone redox systems has motivated a great deal of research evaluating the electrochemical behavior of the quinone–hydroquinone systems.^{12–24} Most investigations focus on the reduction kinetics and mechanisms in protic and aprotic media,^{12–14} determination of the relationship between chemical structure and redox potentials,^{15–19} and how adding proton donor species influences the electro-reduction mechanisms.^{20–24}

In this paper, we concentrated on determining the favored site of electron acceptance within the asymmetrically substituted *p*-naphthoquinones. We previously used electrochemical and theoretical methods to show that, for the 2-[(*R*-phenyl)amino]-1,4-naphthalenediones (PANs), the first electron transfer corresponds to the reduction of the α -carbonyl to the amino group (carbonyl, C₁–O₁, Table 1). Here, we extended the investigation to another series of quinones, the 2-*R*-5*H*-benzo[*b*]carbazole-6,11-diones (BCDs) (Table 1). The purpose of this study was to determine the precise electron acceptance site of the BCD molecules and to establish a relationship between molecular structure and the reduction target of the electrons for the two quinone series PANs and BCDs.

We synthesized five BCD derivatives on which voltammetric studies in acetonitrile and analyses of their molecular geometry using computational chemistry were performed. The hybrid B3LYP functional was employed to optimize the molecular geometry for the BCDs studied. We determined the Wiberg bond indexes (WBIs), natural charges, densities at critical bond points, Laplacians, and ellipticities for each of the derivatives. The correlation between the electrochemical and theoretical data, for both the PAN¹⁹ and the BCD compounds, showed that the presence of intramolecular hydrogen bonds (O₁⋯H–N) plays an important role in determining the acceptance

Table 1. Structures and Relevant Spectroscopic Data for the BCDs and for the PANs Studied in This Work

Structure	Compound	R	x-band	y-band
			λ_{\max}^a (log ϵ_{\max}^b)	λ_{\max}^a (log ϵ_{\max}^b)
	<i>p</i> -MeOPAN	CH ₃ O	271(4.62)	480(3.67)
	<i>p</i> -MePAN	CH ₃	272(4.60)	473(3.78)
	PAN	H	272(4.57)	466(3.78)
	<i>p</i> -COMePAN	COCH ₃	302(4.32)	459(3.69)
	<i>p</i> -CF ₃ PAN	CF ₃	271(4.55)	452(3.71)
	MeOBCD ^c	CH ₃ O	271(4.54)	430(3.87)
	MeBCD	CH ₃	271(4.65)	402(3.93)
	BCD	H	270(4.49)	381(3.76)
	COMeBCD ^c	COCH ₃	266(4.49)	368(3.69)
	CF ₃ BCD ^c	CF ₃	279(4.61)	348(3.80)

^a The UV–vis spectra were determined using EtOH as solvent, and the λ_{\max} values are in nanometers. ^b ϵ_{\max} values are in L mol^{–1} cm^{–1}. ^c These compounds have not been previously described; see the Experimental Section.

site of the first electron in the electrochemical reduction of the quinone system. The use of acetonitrile as solvent in the electrolytic medium was particularly important since the quinones and their corresponding anions are solvated far less efficiently²⁵ than in water, and consequently, the intramolecular hydrogen bonds are more important.²⁶ Moreover, aprotic solvents mimic nonpolar environments of the cell where much of the biological electron transfer occurs.²⁷

The biological activity of quinoid compounds depends not only on the ability of the quinone system to accept electrons, but also on the site of electron acceptance within the quinone itself.¹¹ Determining acceptance sites could provide valuable information on the mechanisms of biological activity and aid in designing new molecules with greater and more efficient biological activity than those currently available.

Results and Discussion

Spectroscopy. In ethanol, all the PANs and BCDs studied produced very similar electronic absorption spectra with a band (x) in the 266–302 nm region (log ϵ = 4.32–4.65) and a very broad, low energy band (y) in the visible region centered between 452 and 480 nm (log ϵ = 3.67–3.78) for PANs and 348 and 430 nm (log ϵ = 3.69–3.93) for BCDs (Table 1). These bands are due to π – π^* electronic transitions of the aromatic systems in the molecules. This was confirmed by the fact that both bands underwent a bathochromic shift when the polarity of the

(11) Baum, R. M. *Chem. Eng. News* **1987**, 19–21.

(12) (a) Chambers, J. Q. In *The Chemistry of the Quinoid Compounds*; Patai, S., Rapport, Z., Eds.; Wiley: New York, 1988; Vol. II, Chapter 12, pp 719–757; 1974; Vol. I, Chapter 14, pp 737–791. (b) Evans, D. H. Carbonyl Compounds. *Encyclopedia of Electrochemistry of the Elements*; Marcel Dekker: New York, 1978; Vol. XII, Chapter 1, p 3. (c) Laviron, E. *J. Electroanal. Chem.* **1986**, 208, 357–372.

(13) Peover, M. E. In *Electroanalytical Chemistry*; Bard, A. J., Ed.; Dekker: New York, 1967; pp 1–51.

(14) Kolthoff, I. M.; Lingane, J. J. *Polarography*, 2nd ed.; Interscience: New York, 1952; Vols. I and II.

(15) (a) Zuman, P. *Substituent Effects in Organic Polarography*; Plenum Press: New York, 1967; Chapters I–III and VIII. (b) Zuman, P. *Collect. Czech. Chem. Commun.* **1962**, 27, 2035–2057.

(16) Li, C.-Y.; Caspar, M. L.; Dixon, D. W. *Electrochim. Acta* **1980**, 25, 1135–1142.

(17) Glezer, V.; Turovska, B.; Stradins, J.; Freimanis, J. *Electrochim. Acta* **1990**, 35 (11/12), 1933–1940.

(18) Suresh Babu, S.; Subba Reddy, G. V.; Rajendra Kumar Reddy, P.; Jayarama Reddy, S. *U. Scientist Phyl. Sci.* **1995**, 7 (1), 43–53.

(19) Aguilar-Martínez, M.; Cuevas, G.; Jiménez-Estrada, M.; González, I.; Lotina-Hennsen, B.; Macías-Ruvalcaba, N. *J. Org. Chem.* **1999**, 64, 3684–3694.

(20) Given, P. H.; Peover, M. E. *J. Chem. Soc.* **1960**, 385–393.

(21) Eggins, B. R.; Chambers, J. Q. *J. Electrochem. Soc.* **1970**, 117 (2), 186–192.

(22) (a) Ortiz, J. L.; Delgado, J.; Baeza, A.; González, I.; Sanabria, R.; Miranda, R. *J. Electroanal. Chem.* **1996**, 411, 103–107. (b) González, F. J.; Aceves, J. M.; Miranda, R.; González, I. *J. Electroanal. Chem.* **1991**, 310, 293–303.

(23) Gupta, N.; Linschitz, H. *J. Am. Chem. Soc.* **1997**, 119, 6384–6391.

(24) Uno, B.; Okumura, N.; Goto M.; Kano, K. *J. Org. Chem.* **2000**, 65, 1448–1455.

(25) Although dipolar aprotic solvents ordinarily have large dipole moments, they are relatively ineffective at solvating the negative ions by dipole interactions because the positive ends of the dipole are usually buried in the middle of the molecule.²⁶

(26) Lowry, T. H.; Richardson, K. S. *Mechanism and Theory in Organic Electrochemistry*; Harpenter & Row Publishers: New York, 1987; Chapter 2. (b) Kosower, E. M. *An Introduction to Physical Organic Chemistry*; John Wiley & Sons: New York, 1986; Part 2.

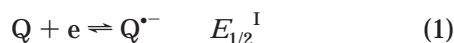
(27) (a) Li, C.-Y.; Jenq, J. *Electrochim. Acta* **1991**, 36, 269–276. (b) Crawford, P. W.; Gross, J.; Lawson, K.; Cheng, C. C.; Dong, Q.; Liu, D. F.; Luo, Y. L.; Szczepankiewicz, B. G.; Heathcock, C. H. *J. Electrochem. Soc.* **1997**, 144, 3710–3715. (c) Jezziorek, D.; Ossowski, T.; Liwo, A.; Dyl, D.; Nowacka, M.; Woźnicki, W. *J. Chem. Soc., Perkin Trans. 2* **1997**, 229–236; (d) Weiss, H.; Friedrich, T.; Hofhaus, G.; Preis, D. *Eur. J. Biochem.* **1991**, 197, 536. (e) Ashnagar, A.; Bruce, J. M.; Dutton, P. L.; Prince, R. C. *Biochim. Biophys. Acta* **1984**, 801, 351–359. (f) Crawford, P. W.; Carlos, E.; Ellegood, J. C.; Cheng, C. C.; Dong, Q.; Liu, D. F.; Luo, Y. L. *Electrochim. Acta* **1996**, 41, 2399–2403.

solvent was increased (i.e., MeBCD in acetonitrile shows two bands at 267 and 392 nm, while in ethanol these bands are located at 271 and 402 nm). Some quinones show specific absorptions originating from the substituent; these will not be discussed in this paper.

Table 1 shows that, in the BCDs, molecular closure gives rise to the aromatic indole system, causing a shift to shorter wavelengths for the γ -band. These results indicate that, in the PAN series, displacement of the electronic density between the naphthoquinone ring and the substituted aniline is more efficient than between the indole and the naphthoquinone in the BCDs, since the indole system apparently behaves as an independent group.

It is well-known that both the electron-accepting and electron-donating substituents allow the general π - π^* bands contributed from the HOMO-LUMO configuration to be shifted to longer wavelengths.²⁸ However, we found that, for both series of compounds, the λ_{\max} for the γ -band shows an interesting shift, which depends on the substituent. The electron-donor groups produced a change in the absorption toward longer wavelengths, while the electron-accepting groups caused the opposite effect (Table 1). These changes seem more important in the BCD molecules.

Electrochemistry. Voltammetric studies of all the PANs and BCDs evaluated here (Table 1) were performed at 25 °C using a glassy carbon working electrode and 0.1 M tetraethylammonium tetrafluoroborate in acetonitrile as the electrolytic medium. The BCDs were less soluble in acetonitrile than their PAN counterparts. BCDs containing electron-accepting substituents were less soluble than BCDs with electron-donor groups. For all PAN and BCD compounds, the voltammograms, recorded in the potential range from +433 to -2233 mV, produced two reversible waves. The first wave is attributed to the addition of an electron to the quinone (Q) to produce a semiquinone radical anion ($Q^{\cdot-}$) and the second one to the subsequent addition of an electron to the semiquinone radical anion, producing a dianion hydroquinone (Q^{2-})¹²⁻¹⁴ (eqs 1 and 2).



From the voltammetric curves, we evaluated the following parameters: (a) half-wave potentials, $E_{1/2} = (E_{pa} + E_{pc})/2$ corresponding to waves I and II, where E_{pa} and E_{pc} correspond to the anodic and cathodic peak potentials, respectively, (b) the values of $\Delta E_{1/2} = E_{1/2}^I - E_{1/2}^{II}$, where $E_{1/2}^I$ and $E_{1/2}^{II}$ correspond to half-wave potentials of waves I and II, respectively, and (c) the equilibrium constants for the comproportionation reaction ($\ln K$) (Table 2) (see below). Table 2 also includes the voltammetric parameters previously obtained for naphthoquinone (NQ) for comparison.¹⁹

Effect of Chemical Structure and Electronic Effect of the Substituent Groups on $E_{1/2}$ Potentials. Both reduction waves, Q to $Q^{\cdot-}$ (wave I) and $Q^{\cdot-}$ to Q^{2-} (wave II), produced more negative $E_{1/2}$ potentials for the PANs and BCDs than for the naphthoquinone (NQ)

Table 2. Voltammetric Parameters^a for PANs^b and BCDs

compd	$E_{1/2}$ (mV) ($(E_{1/2}^I + E_{1/2}^{II})/2$)		$\Delta E_{1/2}$ (mV) ($E_{1/2}^I - E_{1/2}^{II}$)	$\ln K^c$
	wave I	wave II		
NQ	-1036	-1495	459	17.9
<i>p</i> -MeOPAN	-1236	-1809	573	22.3
<i>p</i> -MePAN	-1216	-1773	557	21.7
PAN	-1209	-1685	476	18.5
<i>p</i> -COCH ₃ PAN	-1126	-1554	428	16.7
<i>p</i> -CF ₃ PAN	-1147	-1602	455	17.7
MeOBCD	-1203	-1788	585	22.8
MeBCD	-1208	-1796	588	22.8
BCD	-1188	-1778	590	22.9
COCH ₃ BCD	-1078	-1738	660	25.7
CF ₃ BCD	-1057	-1727	670	26.1

^a Determined by cyclic voltammetry at 100 mV/s using a glassy carbon working electrode and Pt counter electrode. The potentials are given with respect to the Fc^+/Fc redox couple. Because of the insolubility of many of the quinones in the electrolytic medium, not all of them were used at the same concentrations. ^b The $E_{1/2}$ data for the compounds of the PAN series were obtained from ref 19. ^c Logarithms of the equilibrium constant of eq 7 producing the radical anion ($\ln K = (F/RT)(E_{1/2}^I - E_{1/2}^{II})$).

molecule as shown in Table 2. Such behavior indicates that substitution of the different anilines in the *p*-naphthoquinone nucleus (PAN system) or fusion of the *p*-naphthoquinone ring with an indole 5-substituted (BCD system) (Table 1) increases electron density (ρ) on the quinone ring. Such an increase is explained by the fact that, in these molecules, the lone pair of nitrogen in the α -position to the C₁-O₁ carbonyl group is displaced toward the enone system of the quinone as shown in Figure 1 (structures I and IV). For a single substituent group, the $E_{1/2}$ potentials corresponding to the first reduction wave were less negative for the BCDs than for the PANs. With the exception of MeOBCD, the $E_{1/2}$ potentials corresponding to the second electron transfer (wave II) present the opposite effect (Table 2).

For PAN and its derivatives, as well as for the BCD series, introduction of electron-donor groups (i.e., -OMe and -Me) displaced $E_{1/2}$ potentials for the first reduction wave toward a more negative region than the $E_{1/2}$ potentials corresponding to the parent compound (PAN or BCD). Introduction of electron-accepting substituents (-COMe and -CF₃) changed the $E_{1/2}$ potentials to a less negative region (Table 2). Electron-accepting groups reduced the electron density of the electroactive group, facilitating the reduction process, while electron-donor groups have the opposite effect. The degree of positive or negative change is directly related to the magnitude of the electronic effect of the substituent group. Thus, for the BCDs, the molecule with a substituted -CF₃ group, which has an electron-accepting effect slightly greater than that of the -COMe group ($\sigma_p = 0.54$ and 0.50, respectively),²⁹ results in a greater positive change for $E_{1/2}$ of both reduction waves than that observed for the molecule substituted with a -COMe group. The analogous situation occurs in PAN derivatives for the electron-donor groups. The *p*-MeOPAN molecule undergoes a greater negative change than *p*-MePAN, agreeing with the Hammett σ_p constants for these substituent groups (for -OMe $\sigma_p = -0.27$, and for -Me $\sigma_p = -0.17$).²⁹ Nonetheless, for the BCD series, when R = -OMe, both reduction waves present a less negative change than that observed in the MeBCD (Table 2). Therefore, in this

(28) Silverstein, R. M.; Clayton Bassler, G.; Morrill, T. C. *Spectroscopic Identification of Organic Compounds*, 5th ed.; John Wiley & Sons: New York, 1991; Chapter 7, pp 289-316.

(29) Hansch, C.; Leo, A.; Taft, R. W. *Chem. Rev.* **1991**, *91*, 165-195.

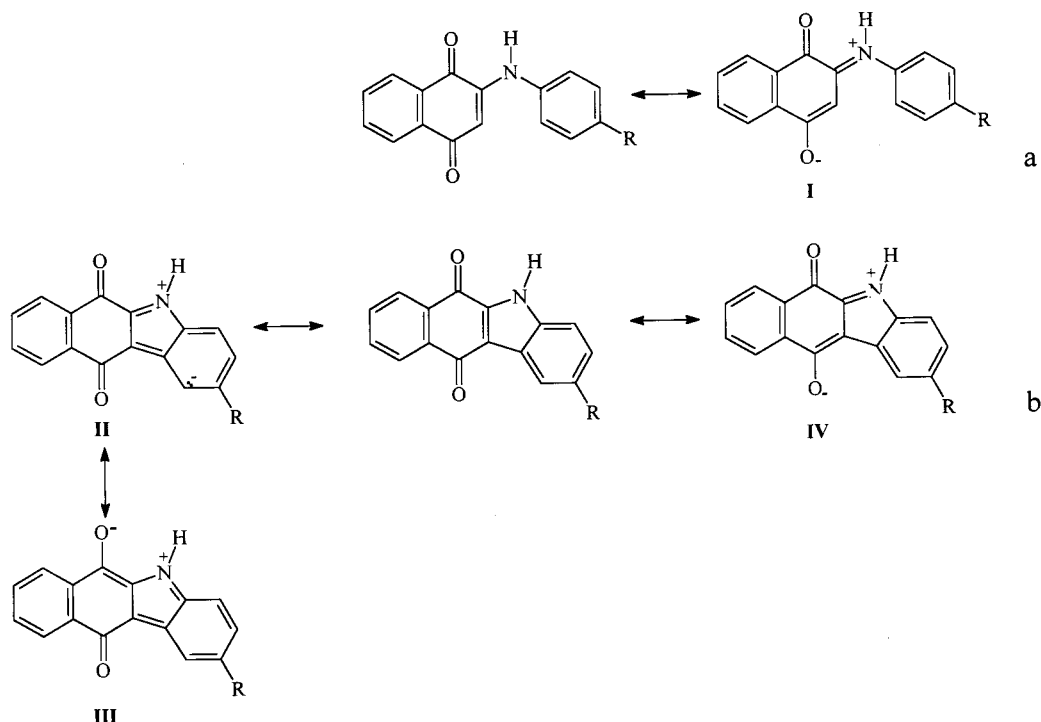


Figure 1. Resonant hybrids for (a) PANs and (b) BCDs, showing displacement of the lone pair of the nitrogen toward the quinone ring (structures **I** and **IV**) and toward the indole ring in the BCDs (structures **II** and **III**).

system, the link between the quinone ring and the substituted aromatic ring (C_3-C_6' bond) results in the inductive effect of the substituents being felt in the quinone system. Since $-OMe$ is an electron-accepting group by inductive effect ($\sigma_m = 0.12$), the magnitude of the negative change observed indicates that there is resonance competition between the electron-donor effect and the inductive electron-acceptor effect. Comparing the $E_{1/2}$ for MeOBCD with that of BCD demonstrates that the electron-donor effect predominates.

To establish a quantitative relationship of the magnitude of the effect of substituents on the electrochemical reduction of the PANs and the BCDs, we correlated the Hammett σ_p constants of the different substituent groups with the $\Delta E_{1/2}$ potentials of waves I and II as presented in eqs 3–6.¹⁵

for the PAN series

$$\Delta E_{1/2}(\text{wave I}) = (123 \pm 7.6)\sigma_p + 7.5 \pm 1.3$$

$$(n = 5, r^2 = 0.9517) \quad (3)$$

$$\Delta E_{1/2}(\text{wave II}) = (277 \pm 6.4)\sigma_p + 32.9 \pm 2.1$$

$$(n = 5, r^2 = 0.9323) \quad (4)$$

for the BCD series

$$\Delta E_{1/2}(\text{wave I}) = (190 \pm 8.7)\sigma_p + 18.4 \pm 2.3$$

$$(n = 5, r^2 = 0.9621) \quad (5)$$

$$\Delta E_{1/2}(\text{wave II}) = (80 \pm 6.0)\sigma_p + 2.3 \pm 0.8$$

$$(n = 5, r^2 = 0.9323) \quad (6)$$

Here $\Delta E_{1/2}$ is the difference in half-wave potentials between the substituted quinone and the parent reference compound PAN or BCD. To assess correctly the effect of the substituents on the second reduction peak, σ_{p^-} constants for radical anions should be used. Since the σ_{p^-} values for the studied compounds are not

available, we used the standard Hammett values as an approximation of the substituent effect, as suggested by Hammett ($\sigma_p = -0.27$ ($-OMe$), -0.17 ($-Me$), 0 (H), 0.5 ($-COMe$), 0.54 ($-CF_3$)).²⁹

The sensitivity of the electrochemical reduction to the electronic effect of the substituents, characterized by the values of the slope¹⁵ in eqs 3–6, indicates that even when there is no direct conjugation between the substituent group and the quinone system in either of the two series of compounds, electrochemical reduction of the quinone system is sensitive to electronic perturbation of the substituents. The positive values of the slopes illustrate that an increase in the electron attraction of the substituent facilitates the reduction of the quinone. Equations 3 and 4 show that, for the PAN series, the reduction of Q to $Q^{\cdot-}$ (wave I) is less susceptible to the effect of the substituents than is the reduction of $Q^{\cdot-}$ to Q^{2-} (wave II) (slope values 123 ± 7.6 and 277 ± 6.4 mV, respectively). In previous studies¹⁹ we found that, for this system, the first electron transfer corresponds to the reduction of α -carbonyl to the amino group (C_1-O_1 carbonyl), and wave II is associated with reduction of the C_4-O_2 carbonyl. Thus, the greater susceptibility of the second wave to the electronic effect of the substituent in the PAN series occurs since, in these molecules, displacement of the electron pair of the amine nitrogen mainly affects the electron density of the C_4-O_2 carbonyl (Figure 1, structure **I**). The magnitude of such a displacement has been shown to be influenced strongly by the type of substituent group present in the phenyl ring.¹⁹ Surprisingly, for BCDs we observe that the first wave is more susceptible to the effect of the substituents than the second wave, slope values 190 ± 8.7 and 80 ± 6.0 mV, respectively (eqs 5 and 6). We explain this behavior in the section below on theoretical calculations.

Effect of the Chemical Structure and Electronic Effect of the Substituent Groups on Radical Anion Stability. Two successive well-separated reduction waves,

corresponding to one electron charge transfer each, are associated with the presence of stable radical anions. To obtain a quantitative measurement of the stability of the radical anions, we should refer to the equilibrium constants for the disproportionation reaction (inverse of eq 7); however, this type of reaction, probably because of the extremely low equilibrium constants, is not usually mentioned in the literature.^{17,30,31} Instead, the opposite reaction, comproportionation,^{32,33} which involves the reaction of Q^{2-} with Q to yield $Q^{\bullet-}$ (eq 7), is discussed more frequently. In this work we discuss the stability of the radical anions ($Q^{\bullet-}$) in terms of the equilibrium constants K of the comproportionation reaction. The values of $\ln K$ were calculated from the difference between the potentials of the first and the second charge transfers as indicated in eq 8, where the K values are expressed as shown in eq 9. Thus, a high value of $\ln K$ means that the $Q^{\bullet-}$ is not prone to disproportionation; hence, it is more stable.



$$\ln K = \frac{F}{RT}(E_{1/2}^I - E_{1/2}^{II}) \quad (8)$$

$$K = \frac{[Q^{\bullet-}]^2}{[Q][Q^{2-}]} \quad (9)$$

Since the $E_{1/2}$ values for all the quinones were evaluated under the same experimental conditions, the observed changes in the $\ln K$ values shown in Table 2 can only be associated with the structural modifications of the molecules, such as the joining of the *p*-naphthoquinone ring with an indolic 5-substituted ring (BCDs), or with *p*-substituted aniline (PANs), as well as the electronic effect of the substituents.

As shown in Table 2, the BCDs have higher $\ln K$ values than the PANs. This indicates that the radical anion formed in the BCDs is more stable, toward disproportionation, than the radical anion obtained for the PAN derivatives. One would expect the stability constants of $-COMe$ and $-CF_3$ compounds to be greater than those of $-OMe$ and $-Me$ compounds because of the strong electron-accepting capacity of $-COMe$ and $-CF_3$ groups. However, this behavior was observed only for the BCD compounds (Table 2). The opposite effect was seen for the PAN derivatives since, in this case, substitution of electron-donor groups leads to more stable radical anions than when R is an electron-accepting group (Table 2). The greater stability of $Q^{\bullet-}$ for the BCDs compared to the PANs is due to the fact that more resonant forms participate in stabilization of the radical anion in the BCDs than in the PANs. This is explained by the fact that the extra electron can be displaced over the four rings of the molecule, regardless of the type of substituent in R . In the PAN system, however, the degree of

displacement of the radical anion is directly related to the type of the substituent in R . Electron-donor groups favor displacement of the free pair of electrons in the nitrogen toward the quinone system (Figure 2, structure **VI**), while electron-accepting groups facilitate displacement of the electron density of the nitrogen toward the aniline system (Figure 2, structure **VII**).¹⁹ Thereby, if R is an electron-accepting group, the extra electron, initially located at C_1 , can become stabilized only over the naphthoquinone ring¹⁹ (Figure 2, structures **VII–X**). If R is an electron-donor group, the radical anion can become stabilized not only over the naphthoquinone ring, but also over the aniline ring, as shown in structures **XI** and **XII** of Figure 2. This behavior explains the apparent inconsistency that, for the PAN molecules, electron-donor groups increase the radical anion stability.

Theoretical Calculations. To explain the experimental observations described above, we performed a complete optimization of the molecular geometry for the compounds MeOBCD, MeBCD, BCD, ClBCD, COMeBCD, CF_3 BCD, CNBCD, and NO_2 BCD as molecular models corresponding to the BCD series. These studies were performed within the framework of the density functional theory³⁴ with the B3LYP hybrid functional, using a double ζ split valence basis set as implemented in Gaussian 94 (G94) programs.³⁵ The relevant geometric data are included in Table S1 of the Supporting Information. Table S2 (Supporting Information) shows the WBIs, calculated with the natural bond orbital (NBO) program³⁶ at the B3LYP/6-31G(d,p) level of theory, as well as the densities of the relevant critical points (ρ), the Laplacians ($\nabla^2\rho$), and the ellipticities (ϵ) determined using the AIM program.³⁷ Table S3 (Supporting Information) includes natural charges, and Table 3 shows the energies of the highest occupied molecular orbital (HOMO) and the lowest unoccupied molecular orbital (LUMO), the hardness (η), and the total energy of the molecules (E_{total}). Numeration for the different atoms in the PAN and BCD molecules is shown in Table 1.

Geometric data included in Table S1 (Supporting Information) illustrate that none of the BCD molecules studied deviate from planarity, allowing the nitrogen atom to maintain a p-type orbital (determined by NBO analysis, vide infra) with an electron pair that allows it to participate in conjugation with the benzene ring and with the quinone rings. The analysis of the bond distances, WBIs, ρ values, and $\nabla^2\rho$ values, for the $C_1-N-C_2-C_1-O_1$ fragment (Tables S1 and S2) indicates that, in the BCD system, the electronic density of the indole system is also displaced toward the C_1-C_2

(30) Jensen, B. S.; Parker, V. D. *J. Am. Chem. Soc.* **1975**, *97*, 5211–5217.

(31) Leventis, N.; Elder, I. A.; Gao, X.; Bohannan, E. W.; Sotiriou-Leventis, C.; Rawashdeh, A. M. M.; Overschmidt, T. J.; Gaston, K. R. *J. Phys. Chem. B* **2001**, *105*, 3663–3674.

(32) (a) Kitagawa, T.; Toyoda, J.; Nakasuji, K.; Yamamoto, H.; Murata, I. *Chem. Lett.* **1990**, 897–900. (b) Illescas, B.; Martin, N.; Segura, J. L.; Seoane, C. *J. Org. Chem.* **1995**, *60*, 5643–5650.

(33) (a) Leventis, N.; Gao, X. *J. Electroanal. Chem.* **2001**, *500*, 78. (b) Amatore, C.; Bonhomme, F.; Bruneel, J.-L.; Servant, L.; Thouin, L. *J. Electroanal. Chem.* **2000**, *484*, 1. (c) Rongfeng, Z.; Evans, D. H. *J. Electroanal. Chem.* **1995**, *385*, 201.

(34) Malkin, V. G.; Malkina, O. L.; Eriksson, L. A.; Salahub, D. R. In *Modern Density Functional Theory. A Tool for Chemistry*; Seminar, J. M., Politzer, P., Eds.; Elsevier: Amsterdam, 1995.

(35) Frisch, M. J.; Trucks, G. W.; Schlegel, H. B.; Gill, P. M. W.; Johnson, B. G.; Robb, M. A.; Cheeseman, J. R.; Keith, T.; Petersson, G. A.; Montgomery, J. A.; Raghavachari, K.; Al-Laham, M. A.; Zakrzewski, V. G.; Ortiz, J. V.; Foresman, J. B.; Cioslowski, J.; Stefanov, B. B.; Nanayakkara, A.; Challacombe, M.; Peng, C. Y.; Ayala, P. Y.; Chen, W.; Wong, M. W.; Andres, J. L.; Replogle, E. S.; Gomperts, R.; Martin, R. L.; Fox, D. J.; Binkley, J. S.; Defrees, D. J.; Baker, J.; Stewart, J. P.; Head-Gordon, M.; Gonzalez, C.; Pople, J. A. *Gaussian 94*, revision D.4; Gaussian, Inc.: Pittsburgh, PA, 1995.

(36) NBO 4.0; Glendening, E. D.; Badenhoop, J. K.; Reed, A. E.; Carpenter, J. E.; Weinhold, F., Theoretical Chemistry Institute, University of Wisconsin, Madison, WI, 1994. Reed, A. E.; Weinstock, R. B.; Weinhold, F. *J. J. Chem. Phys.* **1985**, *83*, 735–746. Reed, A. E.; Weinhold, F. *J. J. Chem. Phys.* **1985**, *83*, 1736–1740. Reed, A. E.; Curtiss, L. A.; Weinhold, F. *Chem. Rev.* **1988**, *88*, 899–926.

(37) Biegler-Koenig, F. W.; Bader, R. F. W.; Tang, T. H. *J. Comput. Chem.* **1982**, *3* (3), 317–328.

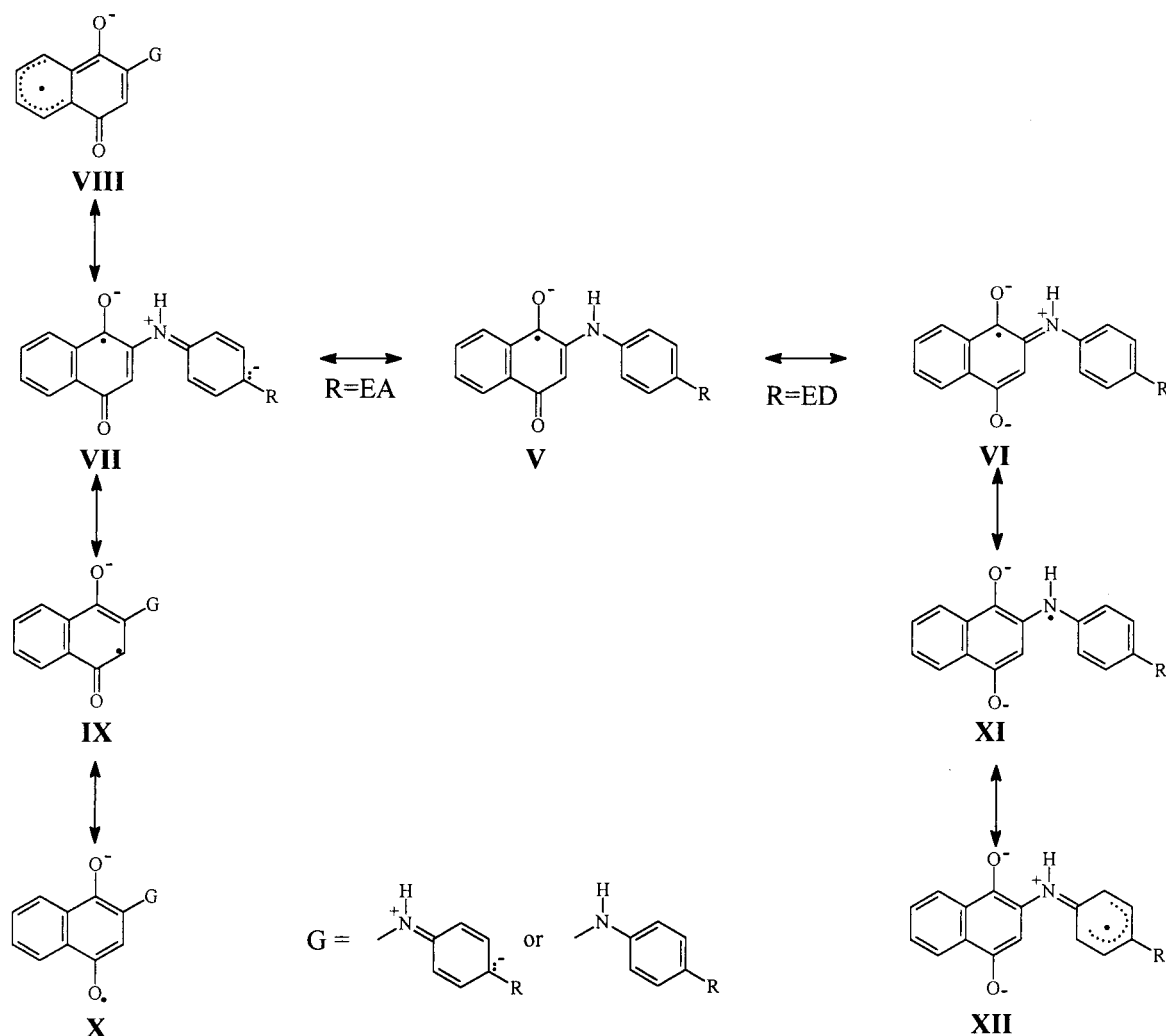


Figure 2. Resonance hybrids showing stabilization of the radical anion of the PANs where R is an electron-donor (ED) group or an electron-accepting (EA) group.

Table 3. Energy of the Frontier Orbitals and Their Neighbors in hartrees for the Quinones MeOBCD, MeBCD, BCD, ClBCD, COMeBCD, CF₃BCD, CNBCD, and NO₂BCD

R	$E_{\text{HOMO}}-1$	E_{HOMO}	E_{LUMO}	$E_{\text{LUMO}}+1$	η	E_{total}
OMe	-0.22924	-0.21073	-0.10089	-0.03873	0.05492	-934.89465
Me	-0.23324	-0.22287	-0.10232	-0.03951	0.06028	-859.69225
H	-0.24061	-0.22672	-0.10383	-0.04103	0.06145	-820.37233
Cl	-0.24220	-0.23481	-0.10989	-0.04797	0.06246	-1279.96543
COMe	-0.24742	-0.23695	-0.11202	-0.05120	0.06247	-973.02320
CF ₃	-0.25618	-0.23934	-0.11280	-0.04990	0.06327	-1154.40724
CN	-0.25625	-0.24632	-0.11775	-0.05515	0.06429	-912.61332
NO ₂	-0.26707	-0.24905	-0.11986	-0.08248	0.06460	-1024.87154

bond as shown in the resonant structure **III** (Figure 1), and not only toward the carbonyl C₄-O₂, as in the PANs (Figure 1, structure **I**). The natural charges shown in Table S3 indicate that the electrophilic character of C₁ decreases when R is an electron-donor group, confirming participation of the resonant form **III** (Figure 1).

Like previous results reported for the PANs,¹⁹ in the BCD series, a bonding pattern also exists for the C₁'-N-C₂-C₃-C₄-O₂ fragment. Increased electron-donor capability in the substituent increases the C₁'-N, C₂-C₃, and C₄-O₂ bond lengths, and decreases the N-C₂ and C₃-C₄ bond lengths. This pattern is explained by participation of the resonant form **IV** presented in Figure 1. The topological analysis of electron density shown in Table S2 established the same pattern in terms of the WBIs, ρ values, and $\nabla^2\rho$ values. However, the magnitude

of the changes in bond lengths is significantly less than changes in bond lengths for the PANs.¹⁹ In the BCDs, there is, therefore, less participation of the free electron pair of the nitrogen toward the quinone system than in the PAN molecules, as demonstrated by the BCD γ -band transition shifting to shorter wavelengths than in the PANs. This behavior is due to the fact that, in the BCDs, the indolic nucleus loses its aromatic character upon conjugating with the C₄-O₂ carbonyl (Figure 1, structure **IV**). The results in Tables S1 and S2 show that even when both fragments C₁'-N-C₂-C₃-C₄-O₂ and C₁'-N-C₂-C₁-O₁ demonstrate sensitivity to the effect of the substituents, the C₁'-N-C₂-C₁-O₁ fragment registers less significant effects as the substituent group changes.

Electronic density analysis of the critical bond points showed that, for the BCD, there was no evidence of

O₁...H–N hydrogen bonding, which had been previously observed for the PAN series.¹⁹ However, the presence of a weak interaction between the proton at C_{5'} and the C₄–O₂ carbonyl oxygen (O₂...H–C_{5'}) was revealed (Figure S1 of the Supporting Information).

Increases in bond distances and decreases in Laplacian and electronic density values for the O₂...H–C_{5'} interaction, observed in the BCDs compared to the corresponding interaction O₁...H–N in the PANs,¹⁹ indicate that the O₂...H–C_{5'} interaction is much weaker than the hydrogen bond O₁...H–N observed in the PANs. It is convenient to mention that we have no experimental evidence for the intramolecular O₂...H–C_{5'} interaction in the BCDs. Furthermore, this hydrogen bond is incompatible with the electronic density delocalization on the indolic system. According to the delocalization of Figure 1 (structure II), the carbon atom C_{5'} accepts a partial negative charge, which decreases the polarization of the C₅–H bond, causing the partial positive charge, required for the hydrogen bond, on that H atom to be diminished. Thus, this hydrogen bond is only a result of theoretical calculations obtained under conditions very different from the experimental conditions. Therefore, in the BCDs the absence of the O₁...H–N interaction provokes the possibility of polarizing the C₁–O₁ carbonyl to be lost, so access of the first electron to C₁ is hindered. We emphasize that, for the BCDs, both the natural charge of the C₄ carbon and the Laplacian value for the C₄–O₂ bond are more positive than those corresponding to the C₁ carbon and the C₁–O₁ carbonyl, indicating that, in this system, the C₄–O₂ carbonyl has a more electrophilic character than the C₁–O₁ carbonyl. Thus, the greater electrophilic character of the C₄–O₂ carbonyl indicates that, for the BCD systems, the first electron transfer corresponds to the reduction of the C₄–O₂ carbonyl and not the C₁–O₂ carbonyl, as is the case for the PANs.¹⁹

Analysis of frontier molecular orbitals supports this scheme since in all the BCDs, the LUMO is located in the Rydberg orbital located at C₄, while for the PANs, the LUMO is found at C₁. In addition, the good linear relationships between the LUMO energy level (E_{LUMO}) and the $E_{1/2}$ potentials for the first reduction wave (eqs 10 and 11) confirm the fact that, in these molecules, the first electron addition occurs at the LUMO.

for the BCD series

$$E_{1/2}(\text{wave I}) = -475E_{\text{LUMO}}(\text{eV}) - 2518$$

$$(n = 5, r^2 = 0.9801) \quad (10)$$

for the PAN series

$$E_{1/2}(\text{wave I}) = -173E_{\text{LUMO}}(\text{eV}) - 1708$$

$$(n = 5, r^2 = 0.9670) \quad (11)$$

The values of the slopes in eqs 10 and 11 also agree with the susceptibility to the effect of the substituents previously seen in the linear trends of eqs 3 and 5. Negative values of the slopes in eqs 10 and 11, on the other hand, indicate that when the LUMO energy level increases, the facility of reduction of the quinone molecule decreases. This suggests that the LUMO energy level could be considered an index of the facility of the molecule to accept electrons. On the basis of this fact and considering that the E_{LUMO} values for a single substituent are greater for the BCD derivatives (Table 3) than for the

PAN derivatives,¹⁹ one would expect the BCDs to have more negative $E_{1/2}$ potentials for the first wave than the PAN molecules. However, we observe in Table 2 that this is not true. This suggests that the LUMO energy level is not the only property determining the reactivity of the molecule in accepting electrons. Neither can we attribute the BCD facility in accepting the first electron to the fact that the radical anion of these molecules is more stable than that of the PAN derivatives (Table 2). If this were true, the molecules *p*-MeOPAN, MeBCD, and MeOBCD, which have similar $\ln K$ values, would also present similar $E_{1/2}$ values for wave I, and this was not the case (Table 2). Thus, it is possible to establish that both the LUMO energies for Q and the stability of the radical anions (Q^{•−}) are factors that significantly affect the half-wave potentials for the first reduction transfer (in accordance with the corresponding Nernst equation).

In agreement with this, the energetics of the second reduction step would be associated with the SOMO (singly occupied molecular orbital) of the radical anions and the electronic repulsion in the SOMO, as well as the stability of the dianion hydroquinones. In our work, SOMO energy values were not determined, and this is the reason the relationships with the half-wave potentials of the second wave are not included.

For the substituted BCDs, NBO analysis establishes that, unlike the LUMO difference, which is always found at the C₄ atom, the HOMO is located on different atoms depending on the substituent. For MeOBCD, the HOMO corresponds to an *np*-type orbital of the unshared electron pairs of the –OMe group oxygen. For CF₃BCD, the HOMO corresponds to an *np*-type orbital of the fluoride atoms, for CNBCD, to the *np*-type electron pair of the –CN group nitrogen, for ClBCD, to an unshared electron pair of the chlorine atom, and for BCD and MeBCD, to an *np*-type orbital of the O₁ of the quinone.

We last discuss the molecular orbital interpretation of the optical absorption properties displayed by quinones studied in this work. From data in Table 3, we establish that the energy gap between the LUMO and HOMO is greater for the BCD compounds than for the PAN derivatives,¹⁹ which is in excellent agreement with the experimental values of λ_{max} for the *y*-band. These results suggest that the lower energy absorption band (*y*-band) of BCDs and PANs could result from the HOMO–LUMO electronic transitions. Experimental observations for the BCDs, where the λ_{max} values for the *y*-band are more susceptible to the effect of the substituents than those of the PAN series of compounds, are explained by the fact that, in the BCDs, the LUMO is localized at C₄, whereas for the PANs, it is at C₁, and the C₄–O₂ carbonyl is more susceptible to the effect of the substituents.

Conclusions

We synthesized five BCDs. In the synthetic strategy, the PANs were used as precursors for the BCDs. Cyclic voltammograms of PANs and BCDs exhibited two one-electron reduction waves to form the corresponding radical anion and dianion. In this study the combination of spectroscopic UV–vis data with the molecular orbital quantum-chemical calculations allowed us to establish that closure of the ring in the PAN molecules (connection between C₃ and C₆) that gives rise to the BCD system results in a decrease in the electron density of the quinone system, as well as loss of the hydrogen bond

between the oxygen of the C₁–O₁ carbonyl and the nitrogen atom (O₁···H–N). The decrease in electron density on the naphthoquinone system explains the slightly less negative reduction potentials measured for the first one-electron transfer in the BCDs compared with PANs.

On the other hand, the absence of the interaction O₁···H–N and the delocalization of the electronic density on the carbonyl C₁–O₁ are factors that contributed to diminishing the polarization of the C₁–O₁ carbonyl, indicating that the C₄–O₂ carbonyl must be more electrophilic than the C₁–O₁ carbonyl. Thus, in the BCDs, the first wave corresponds to reduction of the C₄–O₂ carbonyl, as supported by the fact that, in all the BCDs, the LUMO is at C₄, and not at C₁, as observed for the PAN derivatives.¹⁹ From the obtained results, it was possible to establish that the reactivity of the quinones to accept the first electron depends on both the LUMO energy of the quinone and the stability of the radical anion toward the comproportionation reaction.

Greater susceptibility to the effect of the substituents of the *E*_{1/2} potentials of wave I with respect to wave II in the BCDs is due to the fact that the displacement of the unshared electrons of the nitrogen, which depends on the substituent R, mainly modifies the electron density of the C₄–O₂ bond, with less effect on the electron density of the C₁–O₁ bond.

Experimental Section

Synthesis. ¹H and ¹³C NMR spectra (500 and 75 MHz, respectively) were recorded in CDCl₃ using TMS as a reference. Signals of multiplicity are described as follows: s, singlet; d, doublet; t, triplet; dd, doublet of doublets; td, triplet of doublets. Molecular numbering is given in Table 1. Mass spectra (MS) were performed by electron impact with a beam energy of 70 eV. IR spectra were recorded in KBr pellets. Elemental analyses were performed by Galbraith Laboratories, Inc. Melting points are not corrected.

General Procedure for the Preparation of 2-R-5H-benzo[*b*]carbazole-6,11-diones (BCDs). The synthesis and characterization of PAN and its derivatives are described elsewhere.¹⁹ The preparation of BCDs (Table 1) was performed according to Bittner,³⁸ whose method involves oxidative coupling of the corresponding PANs¹⁹ in the presence of palladium(II) acetate. Equal amounts of the corresponding PAN, benzoquinone, and Pd(OAc)₂ in glacial acetic acid were placed in a three-neck, round-bottom flask (equipped with a thermometer and a reflux condenser with a humidity-absorbing trap). The reaction mixture was stirred at reflux temperature (110 °C) under nitrogen for the required reaction time, which varied for the PAN used. The disappearance of the starting material and appearance of the product were monitored by thin-layer chromatography using mixtures of CH₂Cl₂/EtOH. Once the reaction time was completed, the mixture was allowed to cool to room temperature and filtered to eliminate the Pd(0) formed during the reaction. To ensure elimination of all the AcOH, the reaction mixture was evaporated to dryness at reduced pressure. The residual solid was purified by column chromatography using the mixture of solvents mentioned above to give the corresponding benzocarbazolediones. All the compounds obtained by column chromatography were later recrystallized from the appropriate solvent. The preparation of BCD and MeOBCD was performed as described.^{38,39}

2-Methyl-5H-benzo[*b*]carbazole-6,11-dione (MeBCD). Recrystallization from acetone gave a 35.5% yield: mp 257–

260 °C; IR (KBr, cm⁻¹) 3400, 3232, 3070, 2934, 1666, 1592, 1531, 1483, 1433; UV–vis (EtOH; λ_{max}, nm (ε)) 211 (35889), 271 (44790), 401.5 (8556); ¹H NMR (CDCl₃) δ 12.74 (s, 1H, NH), 8.13 (dd, 1H, *J* = 7.2, 1.7 Hz, H₈), 8.016 (dd, 1H, *J* = 2.5, 0.6 Hz, H₅), 8.09 (dd, 1H, *J* = 7.2, 1.7 Hz, H₅), 7.76 (td, 1H, *J* = 7.4, 1.8 Hz, H₇), 7.71 (td, 1H, *J* = 7.4, 1.8 Hz, H₆), 7.46 (d, 1H, *J* = 8.7 Hz, H₂), 7.20 (dd, 1H, *J* = 7.0, 1.5 Hz, H₃), 2.47 (s, 3H, CH₃); ¹³C NMR (CDCl₃) δ 180.13 (C₁), 177.28 (C₄), 134.11 (C₁'), 133.34 (C₇'), 132.91 (C_{8a}'), 132.91 (C_{4a}'), 132.52 (C₄'), 132.24 (C₆'), 128.31 (C₃'), 125.75 (C₈'), 125.53 (C₅'), 124.16 (C₂'), 121.57 (C₆'), 121.56 (C₅'), 116.98 (C₃'), 113.06 (C₂'), 21.11 (CH₃); MS *m/z* 261, 260, 232, 204. Anal. Calcd for C₁₇H₁₁NO₂: C, 78.15; H, 4.24; N, 5.36. Found: C, 77.88; H, 4.17; N, 5.08.

2-Acetyl-5H-benzo[*b*]carbazole-6,11-dione (COMeBCD). Recrystallization from glacial acetic acid gave a 12% yield: mp 265–266 °C; IR (KBr, cm⁻¹) 3430, 3173, 3136, 2926, 2858, 1667, 1639, 1588, 1385; UV–vis (EtOH; λ_{max}, nm (ε)) 205 (11332), 232 (14479), 266 (31135), 368 (4897); ¹H NMR (CDCl₃) δ 13.16 (s, 1H, NH), 8.81 (d, 1H, *J* = 0.9 Hz, H₅), 8.14 (dd, 1H, *J* = 7.0, 1.5 Hz, H₈), 8.10 (dd, 1H, *J* = 7.5, 1.5 Hz, H₅), 7.95 (dd, 1H, *J* = 8.7, 1.8 Hz, H₃), 7.81 (td, 1H, *J* = 7.5, 1.5 Hz, H₆), 7.76 (td, 1H, *J* = 7.5, 1.5 Hz, H₇), 7.60 (d, 1H, *J* = 8.7 Hz, H₂), 2.67 (s, 3H, CH₃); ¹³C NMR (CDCl₃) δ 179.94 (C₁'), 171.15 (C₄'), 140.28 (C₁'), 138.30 (C₄'), 133.74 (C₆'), 132.72 (C₇'), 132.45 (C_{4a}'), 132.35 (C_{8a}'), 125.87 (C₈'), 125.74 (C₅'), 125.74 (C₃'), 124.82 (C₆'), 123.97 (C₅'), 123.25 (C₂'), 118.27 (C₃'), 113.47 (C₂'), 26.289 (CH₃), 196.47 (C=O); MS *m/z* 289, 274, 264, 190. Anal. Calcd for C₁₈H₁₁NO₃: C, 74.73; H, 3.83; N, 4.84. Found: C, 74.45; H, 4.18; N, 4.53.

2-(Trifluoromethyl)-5H-benzo[*b*]carbazole-6,11-dione (CF₃BCD). Recrystallization from nitrobenzene gave a 16% yield: mp 250–252 °C; IR (KBr, cm⁻¹) 3400, 3244, 2920, 1658, 1593, 1475, 1402; UV–vis (EtOH; λ_{max}, nm (ε)) 206 (24943), 226 (18334), 280 (40512), 348 (6360); MS *m/z* 315, 287, 279, 166, 149. Anal. Calcd for C₁₇H₈F₃NO₂: C, 64.77; H, 2.56; F, 18.08; N, 4.44. Found: C, 64.52; H, 2.48; F, 17.48; N, 4.16.

Electrochemical Procedure. Solvent and Supporting Electrolyte. Acetonitrile (AN) was dried overnight with CaCl₂ and purified by distillation on P₂O₅ under vacuum.⁴⁰ Traces of water in the solvent were eliminated by contact with 3 Å molecular sieves in the dark. The absence of the characteristic –OH bands in the IR spectrum confirmed complete elimination of water traces. Tetraethylammonium tetrafluoroborate (Et₄NBF₄) was dried under vacuum at 60 °C.

Electrodes, Apparatus, and Instrumentation. Cyclic voltammograms were performed at 25 °C. A solution of 0.1 M tetraethylammonium tetrafluoroborate in acetonitrile was used as the electrolytic medium. Since the solubility of the aminoquinones in this medium varied, it was not possible to use all the compounds at the same concentrations. Depending on their solubility, the quinone concentrations varied from 0.34 to 0.64 mM. Prior to electrochemical determinations, N₂ was bubbled through all solutions for 60 min. The inert atmosphere was especially critical in this study since dissolved oxygen in solution not only can be reduced at potentials close to the quinone reduction potentials, but also is capable of oxidizing the radical anion generated in the first stage of reduction, as occurs with other quinones.⁴¹

Voltammetric curves were recorded using an electrochemical analyzer interfaced with a personal computer. Measurements were made over a potential range between +433 and –2233 mV with a scan rate of 10–8000 mV/s. Cyclic voltammetry for all the experiments used a three-electrode cell equipped with a 7 mm² glassy carbon working electrode. Prior to measurements, this electrode was cleaned and polished with 0.05 μm alumina, wiped with a tissue, and sonicated in distilled water for 2–4 min. The counter electrode consisted of a platinum wire with a greater area than the working electrode. A saturated calomel electrode (SCE) served as the reference electrode.

(40) Coetzee, J. F.; Cunningham, D. K.; Mc Guire, D. K.; Padmanabhan, A. *Anal. Chem.* **1962**, *34*, 1139–1143.

(41) Wardman, P.; Tai-Shun L.; Sartorelli, A. C. *J. Med. Chem.* **1986**, *29*, 1381–1384.

(38) Bittner, S.; Krief, P.; Massil, T. *Synthesis* **1991**, 215–216.

(39) Luo, Y.-L.; Chou, T.-C.; Cheng, C. C. *J. Heterocycl. Chem.* **1996**, *23*, 113.

Redox potentials for all compounds were obtained by measuring the current i in the working electrode as a function of the potential E (V) vs the SCE. Contact with the reference electrode was made using a Luggin tube filled with electrolytic medium. To establish an internal reference system, ferrocene was added to the studied solutions, and all the redox potentials reported in this study refer to the ferrocenium/ferrocene redox couple (Fc^+/Fc) as recommended by IUPAC.⁴² In this case the potential for the Fc^+/Fc redox couple, determined by voltamperometric studies, was 443 ± 2 mV.

Computational Methods. Complete geometry optimization was performed according to the density functional theory (DFT) using the B3LYP/6-31G(d,p) level with the Gaussian 94 program (G94).³⁵ The functional hybrid B3LYP defines the functional exchange as a Hartree–Fock local linear combination in terms of gradient exchange.⁴³

The exchange functional is combined with a local correlation function with a corrected gradient. The C*EcLYP+(1-C)-*ECVWN correlation functional is used, where LYP is the Lee, Yang, and Parr⁴⁴ correlation functional, which includes both local and nonlocal terms, and VWN is the Vosko, Wilk, and Nusair correlation functional, to provide the local correlation required in excess, since LYP contains a local term essentially

equivalent to VWN.⁴³ The 6-31G(d,p) orbital base used adds polarization functions for heavy atoms and hydrogen. NBO analysis was performed using version 3.1, which is included in G94.³⁶ Densities computed at B3LYP/6-31G(d,p) from the G94 output were used with the AIMPACK³⁷ set of programs to calculate the properties of critical points (cps) in the charge density, ρ values, $\nabla^2\rho$ values, and ϵ values.

Acknowledgment. We thank the Consejo Nacional de Ciencia y Tecnología (CONACYT) for the financial support given via Grant Nos. 28016E and 32420-E, and for a fellowship to N.M.-R., who is also grateful to DGEP for a complementary fellowship. We are grateful to the Dirección General de Servicios de Cómputo Académico (DGSCA), Universidad Nacional Autónoma de México, and to the Escuela de Ciencias Químicas, Universidad La Salle, for their computational support, as well as for the generous gift of supercomputer CPU time. We really appreciate the suggestions and recommendations of the reviewers that improved this work.

Supporting Information Available: Relevant geometry data, Wiberg bond indexes, properties of the relevant critical points, and natural charges for the BCDs (Tables S1–S3 and Figure S1) and complete computational results in the form of **Z**-matrixes with the computed total energies. This material is available free of charge via the Internet at <http://pubs.acs.org>.

JO011083K

(42) Gritzner, G.; Küta, J. *Pure Appl. Chem.* **1984**, *4*, 462–466.

(43) Stephens, P. J.; Devlin, F. J.; Chabalowski, C. F.; Frisch, M. J. *J. Phys. Chem.* **1994**, *98*, 11623–11627. Becke, A. D. *J. Chem. Phys.* **1993**, *98*, 1372–1377, 5648–5652.

(44) Lee, C.; Yang, W.; Parr, R. G. *Phys. Rev.* **1988**, *B37*, 785–789. Miehlich, B.; Savin, A.; Stoll, H.; Preuss, H. *Chem. Phys. Lett.* **1989**, *157* (3), 200–206.